AIAA JOURNAL
Vol. 32, No. 10, October 1994

Asymmetric Vortex Pair in the Wake of a Circular Cylinder

G. Iosilevskii* and A. Seginer†
Technion—Israel Institute of Technology, Haifa 32000, Israel

Stationary configurations of two asymmetric point vortices in the wake of an infinite circular cylinder, spinning or not about its axis, are analytically investigated using an ideal fluid approximation. Four different vortex configurations (patterns) in the wake of a spinning cylinder are found in the case when vortex asymmetry is weak; each configuration is associated with a certain direction of the Magnus force. The qualitative relation between a pattern and a direction of the Magnus force is in agreement with experimental data. Also obtained are asymmetrical vortex configurations in the wake of a nonspinning cylinder.

I. Introduction

THE flowfield developing around an infinitely long circular cylinder in a crossflow was extensively studied over the last century both analytically and experimentally. It is currently a well-known fact that several characteristic flow patterns in the wake of the cylinder are associated with the crossflow Reynolds number Re.[1] In particular, when $6 < Re < 30$ (the Reynolds number is based on the cylinder's diameter, and the ranges cited ar approximate since they can be affected by the roughness of the cylinder's surface), a pair of concentrated vortices is observed in the wake. The vortices are symmetric relative to the direction of the crossflow and equidistant from the cylinder; both the strength and the distance of the vortices from the cylinder increase with the Reynolds number. When Re increases above 30, the vortices may become asymmetric. In this case, a side force (or a Magnus force; hereafter both names will be used synonymously) is exerted upon the cylinder. With a further increase in the Reynolds number, additional pairs of asymmetric vortices are shed from the cylinder. If the cylinder spins about its axis, then the respective wake vortices are inherently asymmetric; both the loci of the vortices and the side force acting on the cylinder depend on the cylinder's spin rate and on the crossflow Reynolds number.[2]

The majority of the analytical studies of the problem were conducted in the framework of the ideal fluid approximation.[3–6] The latter may be summarized as follows. The fluid is assumed inviscid and incompressible; it is postulated that there exists a wake behind the cylinder; it is further postulated that the wake is comprised of several stationary point vortices, the number of the wake vortices deriving from the respective "physical" flow pattern (cf. the previous paragraph). Each of the cited studies addressed different equilibrium configurations of the vortices. Thus, stationary configurations were found for several pairs of symmetric vortices near a circular cylinder,[3,4] for several pairs of symmetric vortices behind an oscillating circular cylinder confined between walls,[5] and for several pairs of symmetric vortices behind a noncircular cylinder.[6]

All of these studies dealt with symmetric vortices behind a nonspinning cylinder. To the best of our knowledge, asymmetric vortices behind either spinning or nonspinning cylinders were never investigated (although the case of a spinning cylinder without wake vortices was solved by Magnus[7] in 1853). This problem is addressed in the present publication.

II. Ideal Fluid Approximation

A. Preliminaries

Consider an infinite cylinder of radius b spinning with angular velocity Ω in a uniform crossflow of an inviscid and incompressible fluid. Let ρ and U be the (uniform) density of the fluid and the (constant) fluid velocity far from the cylinder, respectively. In the following derivations it will prove convenient to make use of nondimensional quantities, having b, U, bU, $2\pi bU$, $2\pi Ub^2$, and ρbU^2 as units of length, velocity, velocity potential, circulation, strength of a dipole, and force per unit length, respectively. The use of nondimensional quantities will be implicitly understood in all of the subsequent derivations, unless explicitly indicated otherwise.

Let K_3 be a right-handed Cartesian coordinate system whose x and z axes coincide with the direction of the flow far from the cylinder and with the axis of the cylinder, respectively. Let $\langle x, y, z\rangle$ be the ordered triple of coordinates of a point in space relative to K_3. Our previous assumption that the crossflow is uniform implies that the flow patterns in two different planes, say $z = z_1$ and $z = z_2$, are congruent. Accordingly, the plane $z = 0$ may be selected as the representative plane in which the flowfield will be investigated.

In the sequel we shall often prefer cylindrical, $\langle r, \theta, z\rangle$, rather than Cartesian, $\langle x, y, z\rangle$, coordinates. We shall assume that those are related by the expressions $x = r\cos\theta$ and $y = r\sin\theta$.

B. Equilibrium Conditions

It is assumed that in the plane $z = 0$ the wake behind the cylinder is represented by N point vortices of circulations $\gamma_1,\ldots,\gamma_N$, located at the respective points $\langle r_1, \theta_1\rangle, \ldots, \langle r_N, \theta_N\rangle$. Outside the centers of these vortices the flowfield is assumed irrotational and thus governed by the Laplace equation. Accordingly, imaging tech-niques[8] may be used to solve the flowfield.

In particular, a spinning cylinder in a crossflow is represented by a dipole of unit strength aligned with the y axis and a vortex of circulation $\gamma_v = \Omega b/U$, both located at the axis of the cylinder. Each vortex in the exterior of the cylinder is supplemented by two image vortices in the interior of the cylinder (see Fig. 1). Of these, one vortex of circulation

$$\gamma_{-j} = -\gamma_j \tag{1}$$

is placed at the (reflection) point

$$\langle r_{-j}, \theta_{-j}\rangle = \langle 1/r_j, \theta_j\rangle \tag{2}$$

whereas the other, of circulation γ_j, is placed at the axis of the cylinder.[8] In Eqs. (1) and (2), j takes on integer values between 1 and N.

With all flow elements collected together, the stream function,[8] describing the flowfield of the cylinder with N vortices, takes on the form

$$\psi(r,\theta) = r\sin\theta - \frac{\sin\theta}{r} - \frac{1}{2}\sum_{j=-N}^{N}\gamma_j \ell n\left|r^2 + r_j^2 + -2rr_j\cos(\theta-\theta_j)\right| \tag{3}$$

Received June 3, 1993; revision received Jan. 31, 1994; accepted for publication Feb. 4, 1994.

*Lecturer, Faculty of Aerospace Engineering.
†Professor, Faculty of Aerospace Engineering. Member AIAA.

where $r_0 \equiv 0$, whereas

$$\gamma_0 = \gamma_v + \sum_{j=1}^{N} \gamma_j \tag{4}$$

is the effective circulation at the cylinder's axis (reflecting both the cylinder's spin and the respective image vortices).

Given a stationary configuration of the wake vortices, the force acting on each vortex has to be zero. By the Kutta-Jukowski theorem,[8] the latter statement implies that the velocity induced at the center of each wake vortex has to be zero. Thus, by taking to zero each of the two velocity components at the center of each wake vortex, one obtains $2N$ equilibrium conditions to relate N circulations and $2N$ coordinates. As there exist no additional equilibrium conditions within the ideal-fluid approximation, this leaves N parameters undetermined.

The radial (v) and the azimuthal (u) velocity components may be obtained by taking the respective derivatives

$$v = \frac{\partial \psi}{r \partial \theta} \quad \text{and} \quad u = -\frac{\partial \psi}{\partial r}$$

of the stream function. The equilibrium conditions may, therefore, be written in the following form. For each $k \in \{1, 2, ..., N\}$,

$$\begin{aligned} v_k(r_1, ..., r_N, \theta_1, ..., \theta_N, \gamma_0, ..., \gamma_N) &= 0 \\ u_k(r_1, ..., r_N, \theta_1, ..., \theta_N, \gamma_0, ..., \gamma_N) &= 0 \end{aligned} \tag{5}$$

where

$$v_k(r_1, ..., \gamma_N) = \left(1 - \frac{1}{r_k^2}\right)\cos\theta_k - \sum_{\substack{j=-N \\ j \neq k}}^{N} \gamma_j \frac{r_j \sin(\theta_k - \theta_j)}{r_k^2 + r_j^2 - 2 r_k r_j \cos(\theta_k - \theta_j)} \tag{6}$$

$$u_k(r_1, ..., \gamma_N) = -\left(1 + \frac{1}{r_k^2}\right)\sin\theta_k + \sum_{\substack{j=-N \\ j \neq k}}^{N} \gamma_j \frac{r_k - r_j \cos(\theta_k - \theta_j)}{r_k^2 + r_j^2 - 2 r_k r_j \cos(\theta_k - \theta_j)} \tag{7}$$

are the respective velocity components at the center of the kth vortex.

C. Magnus Force

To find the force acting on the cylinder, it proves convenient to replace the real x-y plane by a complex plane, where the real and imaginary axes coincide with the x and y axes, respectively. On the complex plane, the location of a point is uniquely defined by the complex number $\zeta = x + iy$, whereas the velocity field is uniquely defined by the derivative of the complex potential $W(\zeta)$ with respect to ζ.[8] For a spinning cylinder with N point vortices in its exterior,

$$W(\zeta) = \zeta + \frac{1}{\zeta} - i \sum_{j=-N}^{N} \gamma_j \ell n(\zeta - \zeta_j) \tag{8}$$

in accordance with Eq. (3).

The x and y components, F_x and F_y, of the force per unit length in the z direction that is exerted on the interior of a contour C are given by the well-known formula,[8]

$$F_x - iF_y = \frac{i}{2} \oint_C \left(\frac{dW}{d\zeta}\right)^2 d\zeta \tag{9}$$

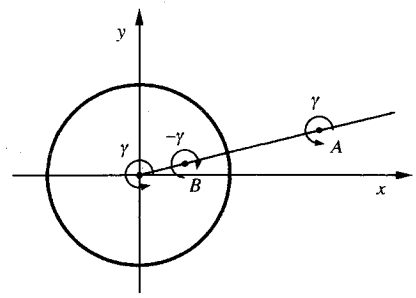

Fig. 1 Each vortex in the exterior of the cylinder (vortex A) is supplemented by two image vortices in the interior of the cylinder: one with the reversed circulation (vortex B) at the reflection point, and the other with the same circulation (as vortex A) at the center of the cylinder.

If the wake vortices occupy their equilibrium positions, and the contour C is selected so as to encircle both the cylinder and its wake vortices, then the force exerted on the interior of C coincides with the force exerted on the cylinder. This statement immediately follows from the equilibrium conditions, by which the force exerted on each wake vortex has to be zero. Thus, by Eqs. (8) and (9),

$$F_x - iF_y = \frac{i}{2} \oint_C \left[1 - \frac{2}{\zeta^2} + \frac{1}{\zeta^4} - 2i \sum_{j=-N}^{N} \frac{\gamma_j(\zeta^2 - 1)}{(\zeta - \zeta_j)\zeta^2} - \sum_{k=-N}^{N} \sum_{j=-N}^{N} \frac{\gamma_j \gamma_k}{(\zeta - \zeta_j)(\zeta - \zeta_k)}\right] d\zeta \tag{10}$$

The integral appearing on the right-hand side of Eq. (10) may be evaluated using the Cauchy formula,[9] by which

$$\oint_C \frac{f(\zeta)}{(\zeta - \zeta_j)^{n+1}} d\zeta = \frac{2\pi i}{n!}\left[\frac{d^n f(\zeta)}{d\zeta^n}\right]_{\zeta = \zeta_j} \tag{11}$$

where ζ_j belongs to the interior of C, f is a meromorphic function[9] on the interior of C, and n is a nonnegative integer. Thus, by Eqs. (1), (4), and (11), Eqs. (10) yields

$$F_x - iF_y = 2\pi i \sum_{j=-N}^{N} \gamma_j = 2\pi i \gamma_0 \tag{12}$$

whence

$$F_x = 0 \tag{13}$$

$$F_y = -2\pi\gamma_0 = -2\pi\left(\gamma_v + \sum_{j=1}^{N} \gamma_j\right) \tag{14}$$

From Eq. (13), it follows that no drag force is exerted upon a spinning cylinder in a crossflow with N stationary vortices in its wake. From Eq. (14), it follows that the respective side force depends upon both the spin rate (γ_v) of the cylinder and the total circulation of the wake vortices. Given that the latter is zero, Eq. (14) yields the classic value of the Magnus force.[8] However, as we are not aware of any physical arguments that may require the total circulation of the wake vortices to be zero, the wake vortices may affect both the magnitude and the direction of the Magnus force.

III. Two-Vortex Wake

A. Notation

Consider the particular case wherein the wake is represented by two vortices only. It will prove convenient to replace the original

six unknowns, being the coordinates and the circulations of the vortices, by the following six linear combinations of the latter:

$\phi = (\theta_1 - \theta_2)/2$ = angular semi-spread between the wake vortices

$\theta = (\theta_1 + \theta_2)/2$ = drift angle of the vortex pair

$R = (r_1 + r_2)/2$ = average distance of the vortices from the center of the cylinder

$\Delta r = (r_1 - r_2)/2$ = radial drift of the vortices

$\gamma_s = (\gamma_1 - \gamma_2)/2$ = "symmetric" circulation of the wake vortices,

$\gamma_a = -(\gamma_1 + \gamma_2)/2$ = "antisymmetric" circulation of the wake vortices.

These are depicted in Fig. 2. Thus, by definition,

$$\gamma_1 = \gamma_s - \gamma_a, \quad \gamma_2 = -\gamma_s - \gamma_a$$
$$\theta_1 = \theta + \phi, \quad \theta_2 = \theta - \phi \tag{15}$$
$$r_1 = R + \Delta r, \quad r_2 = R - \Delta r$$

The six unknowns are related by four equilibrium conditions [deriving from Eq. (5)], whence, any two of them have to be treated as free parameters (namely, they have to be prescribed rather than evaluated in the framework of the theory). Equivalently, the spin rate γ_v of the cylinder may serve as an additional, seventh, parameter, in which case any three out of the seven parameters may be chosen as free parameters. However, regardless of the selection of free parameters, the equilibrium conditions constitute a nonlinear system of equations with respect to the remaining four parameters and are not generally amenable to an analytical solution. Nonetheless, several particular solutions may be obtained after some simplifying assumptions. Two of these solutions will be addressed in the next two sections.

Note that, with one pair of vortices forming the wake of the cylinder, the side force acting on the cylinder is given by a particularly simple expression,

$$F_y = -2\pi\gamma_0 \equiv -2\pi(\gamma_v - 2\gamma_a) \tag{16}$$

immediately following from Eq. (14) by Eq. (15).

B. Symmetric Föppl Solution

Consider first the elementary case of two symmetric vortices behind a stationary cylinder.[3] By the symmetry considerations,

$$\Delta r = \theta = \gamma_a = \gamma_v = 0 \tag{17}$$

and, accordingly, $F_y = 0$ [cf. Eq. (16)]. The remaining three unknowns, namely, $R = r_1 = r_2$, $\phi = \theta_1 = -\theta_2$, and $\gamma_s = \gamma_1 = -\gamma_2$, are related by two independent equilibrium conditions,

$$u_1(R, R, \phi, -\phi, 0, \gamma_s, -\gamma_s) = 0$$
$$v_1(R, R, \phi, -\phi, 0, \gamma_s, -\gamma_s) = 0 \tag{18}$$

thereby leaving one parameter free.

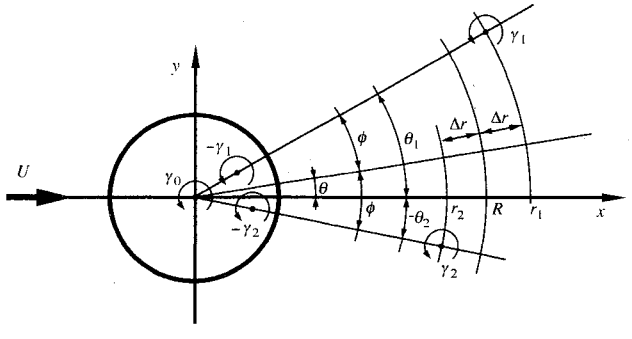

Fig. 2 Flowfield model and notation.

Equations (18) have a well-known (parametric) solution,

$$\gamma_s = \gamma_F(R) \equiv -R\left(1 - \frac{1}{R^2}\right)\left(1 - \frac{1}{R^4}\right)$$
$$\phi = \phi_F(R) \equiv \arcsin\frac{R^2 - 1}{2R^2} \tag{19}$$

commonly associated with the name of Föppl.[3] Additional solution of Eqs. (18), wherein $\phi = \pi/2$,[3] is usually considered physically inadmissible.

C. Weakly Asymmetric Vortices

Given that the cylinder rotates slowly around its axis (or, rather, when this rotation is represented by a weak vortex at the center of the cylinder), it may be expected, subject to a posteriori verification, that the equilibrium positions of the wake vortices will be in the vicinity of the comparable positions corresponding to Föppl's solution [Eq. (17) in conjunction with Eq. (19)]. Consider then the following scheme.

Let R, γ_a, and γ_v be the free parameters. As the perturbations are assumed from Föppl's solution, the choice of R as one of those parameters is natural. The remaining two parameters are chosen in view of their role in determining the Magnus force [cf. Eq. (16)]. For a given R, it is assumed that

$$|\gamma_v| \ll |\gamma_F(R)|, \quad |\gamma_a| \ll |\gamma_F(R)|$$
$$\Delta r \ll R - \frac{1}{R}, \quad |\theta| \ll 1 \tag{20}$$
$$|\Delta\gamma_s| \ll |\gamma_F(R)|, \quad |\Delta\phi| \ll |\phi_F(R)|$$

wherein, by definition,

$$\Delta\gamma_s = \gamma_s - \gamma_F(R), \quad \Delta\phi = \phi - \phi_F(R) \tag{21}$$

Note that since R is a free parameter, it is not possible to determine whether the rotation of the cylinder may affect the distance of the vortices from the cylinder.

For a given R, γ_a, and γ_v, the perturbations Δr, $\Delta\phi$, θ, and $\Delta\gamma_s$ are governed by two syntactically similar pairs of linear equations, of which one is of the form,

$$\left(\frac{\partial u_k}{\partial r_1} - \frac{\partial u_k}{\partial r_2}\right)_F \Delta r + \left(\frac{\partial u_k}{\partial\theta_1} - \frac{\partial u_k}{\partial\theta_2}\right)_F \Delta\phi + \left(\frac{\partial u_k}{\partial\theta_1} + \frac{\partial u_k}{\partial\theta_2}\right)_F \theta$$
$$+\left(\frac{\partial u_k}{\partial\gamma_1} - \frac{\partial u_k}{\partial\gamma_2}\right)\Delta\gamma_s = \left(\frac{\partial u_k}{\partial\gamma_1} + \frac{\partial u_k}{\partial\gamma_2} + 2\frac{\partial u_k}{\partial\gamma_0}\right)_F \gamma_a - \left(\frac{\partial u_k}{\partial\gamma_0}\right)_F \gamma_v$$

with $k \in \{1,2\}$, and the other is obtained by substitution of v_k instead of u_k [these equations immediately follow from Eqs. (5) by Eqs. (15), (20), and (21)]. The solution of these equations is straightforward, although it involves rather lengthy (and somewhat tedious) algebraic derivations. Eventually, one obtains

$$\Delta\gamma_s = \Delta\phi = 0$$
$$\Delta r = \frac{R^4(R^2-1)^2}{2(3R^6+3R^4-3R^2+1)}\gamma_v - \frac{R^4(R^6-R^4+2R^2-1)}{(R^2-1)(3R^6+3R^4-3R^2+1)}\gamma_a$$
$$\theta = \frac{R^5(R^2+1)\cos[\phi_F(R)]}{3R^6+3R^4-3R^2+1}\gamma_v - \frac{2R^5(R^6-3R^2-1)\cos[\phi_F(R)]}{(R^4-1)(3R^6+3R^4-3R^2+1)}\gamma_v \tag{22}$$

IV. Results and Discussion

First, consider the case where $\gamma_v \neq 0$. Under these circumstances, Eqs. (16) and (22) may be written, in symbolic forms, as

$$\Delta r = A_r \gamma_v \left(B_r - 2\frac{\gamma_a}{\gamma_v} \right), \quad \theta = A_\theta \gamma_v \left(B_\theta - 2\frac{\gamma_a}{\gamma_v} \right)$$

$$F_y = -2\pi\gamma_v \left(1 - 2\frac{\gamma_a}{\gamma_v} \right)$$

where A_r, A_θ, B_r, and B_θ are some functions of R. [These functions may be easily identified from Eq. (22), but explicit forms are irrelevant for the present discussion.] Thus, for a given R, the ratio γ_a/γ_v determines both the direction of the Magnus force and the sign of the displacements Δr and θ. In fact, the lines

$$(\gamma_a/\gamma_v) = (\gamma_a/\gamma_v)_{\Delta r = 0} \equiv \frac{(R^2-1)^3}{2(R^6 - R^4 + 2R^2 - 1)}$$

$$(\gamma_a/\gamma_v) = (\gamma_a/\gamma_v)_{\theta = 0} \equiv \frac{(R^2-1)(R^2+1)^2}{2(R^6 - 3R^2 - 1)} \tag{23}$$

separate the $<R, \gamma_a/\gamma_v>$ plane into four parts corresponding to four different modes of vortex displacements (cf. Fig. 3). Each mode is associated with a certain direction of the Magnus force.

Data on the wake patterns behind a two-dimensional rotating cylinder are scarce, but the few data that are available[2,10] demonstrate that the Magnus force changes direction from side to side at certain spin rates. This result may be qualitatively explained in the framework of the present theory by a change in the wake mode. Unfortunately, we did not find data that correlate between a wake pattern behind the cylinder and a direction of the Magnus force, and so we are unable to verify our results.

On the other hand, we believe that the relation between the wake pattern and the direction of the Magnus force may provide some qualitative explanation for the phenomenon observed in the "three-dimensional" case. In fact, given a slender cylindrical body at a large angle of incidence, two vortex "sheets" shed from the body, and at a certain distance from it they roll into two concentrated vortices. The intensities of these vortices, as well as their distance from the cylinder, increase as they progress along the cylinder. Far from the edges of the cylinder, the flow pattern in the plane perpendicular to the longitudinal axis of the cylinder resembles the flow pattern corresponding to the case of an infinite cylinder in a cross-flow. Fletcher[11] suggested that the asymmetrical displacement of the centers of the concentrated vortices in the wake of the cylinder, caused by the rotation of the cylinder, have a major role in determining both the amplitude and the direction of the force acting on the cylinder. Fletcher's observations, as depicted in Fig. 8 of his article, show qualitative agreement with modes 2 and 3 depicted in our Fig. 4, thus apparently justifying his assertion.

The particular wake mode cannot be predicted in the framework of an ideal fluid approximation. Nonetheless, some qualitative remarks may be made. The measured magnitudes of the side force exerted on spinning slender bodies at large angles of attack do not exceed those predicted by the classical Magnus theory, i.e., $|F_y| \leq 2\pi\gamma_v$.[11-14] By Eq. (16), this observation bounds the possible values of the circulation ratio γ_a/γ_v to the interval [0, 1]. This renders mode 4 improbable (cf. Fig. 3). On the other hand, most data on the location of the vortices in the wake indicate that their distances from the center of the cylinder do not exceed twice the cylinder radius; this renders mode 1 improbable as well (cf. Fig. 3). Also, the angular displacements of the vortices in modes 1 and 4 are opposite to the sense of the cylinder's rotation, and such a phenomenon was never observed experimentally. This leaves modes 2 and 3 to be the most probable—in agreement with Fletcher's observations.

An important particular case of the suggested solution is when $\gamma_v = 0$ or else when the cylinder is stationary. In this case, Eqs. (22) yield

$$\Delta r = -\frac{R^4(R^6 - R^4 + 2R^2 - 1)}{(R^2-1)(3R^6 + 3R^4 - 3R^2 + 1)}\gamma_a$$

$$\theta = -\frac{2R^5(R^6 - 3R^2 - 1)\cos[\phi_F(R)]}{(R^4-1)(3R^6 + 3R^4 - 3R^2 + 1)}\gamma_a \tag{24}$$

In other words, the vortex pair in the wake of a stationary cylinder may be asymmetric. Such a configuration was observed experimentally,[15] but was never before predicted in the framework of an ideal-fluid approximation.

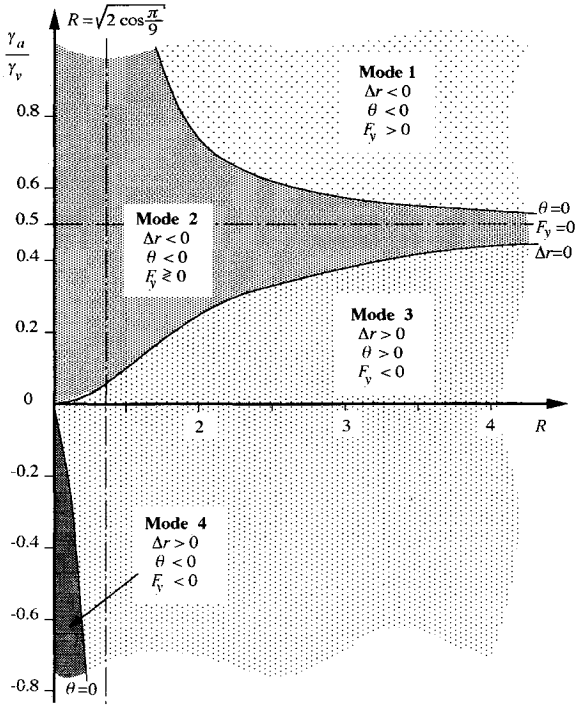

Fig. 3 Lines $\Delta r = 0$ and $\theta = 0$ divide the plane into four parts. Each part is associated with a certain vortex pattern and with a certain direction of the Magnus force.

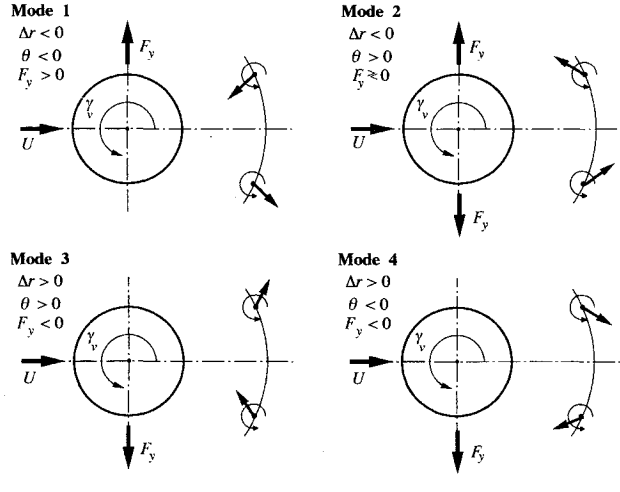

Fig. 4 Spinning cylinder: four different modes of wake vortices displacements may be identified. Each mode is associated with the particular direction of the Magnus force. Modes 1 and 4 seem to be improbable for several reasons discussed in the text. Remaining two modes are in qualitative agreement with experimental data.

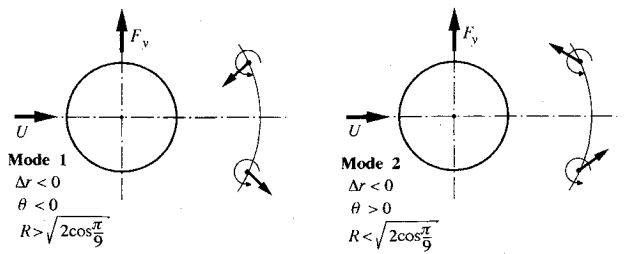

Fig. 5 Stationary cylinder: two different modes of wake vortices displacements may be identified. The transition between the modes occurs at $R \approx 1.37$. The side force always acts in the direction of the closest vortex.

The two wake modes that are possible in this case are shown in Fig. 5. The difference between the modes is in the sign of the angular displacement θ; the transition between the modes occurs at

$$(R)_{\theta=0} = \sqrt{2\cos\frac{\pi}{9}} \tag{25}$$

(the "odd" number comes from the solution of the cubic equation $R^6 - 3R^2 - 1 = 0$). In both modes, the side force on the cylinder acts in the direction of the closest vortex. The global direction of the force, as well as the signs of Δr and θ, depend on the sense of γ_a, whence they cannot be predicted in the framework of this theory.

References

[1]Goldstein, S. (ed.), *Modern Developments in Fluid Dynamics*, Vol. 1, Clarendon Press, Oxford, England, UK, 1938, pp. 62, 63.

[2]Kegelman, J. T., Nelson, R. C., and Mueller, T. J., "Boundary Layer and Side Force Characteristics of a Spinning Axisymmetric Body," AIAA Paper 80-1584, Aug. 1980.

[3]Föppl, L., "Wirbelbewengung Hinter Einen Kreiszylinder," *Sitzung Berichte der Bayerischen Academie der Weissenschaften (Math. Physik)*, 1913, pp. 1–17.

[4]Seath, D. D., "Equilibrium Vortex Positions," *Journal of Aircraft*, Vol. 8, No. 1, 1973, pp. 72–75.

[5]Boasson, M., and Weihs, D., "Symmetric Vortex Shedding from a Cylinder in a Confined Flow," *Israel Journal of Technology*, Vol. 16, Nos. 1/2, 1978, pp. 56–63.

[6]Karou, A., and Weihs, D., "The Stability of Symmetrical Vortices in the wake of Elliptical Cylinders in Confined Flow," *Proceedings of the 26th Israel Annual Conference on Aviation and Astronautics*, 1984, pp. 140–145.

[7]Magnus, F., "Uber die Verdichtung der Gase an der Oberflache Glatter Korper," *Foggendorf Annolen der Physickalsche Chemie*, Vol. 88, No. 1, 1853, pp. 604–610.

[8]Batchelor, G. K., *An Introduction to Fluid Dynamics*, Cambridge Univ. Press, Cambridge, England, UK, 1990, pp. 422, 423, 76, 406, 107, 433, 426.

[9]Churchill, R., *Complex Variables and Applications*, 3rd ed., McGraw-Hill, Tokyo, 1974, pp. 172–174.

[10]Krahn, E., "Negative Magnus Force," *Journal of the Aeronautical Sciences*, Vol. 23, April 1956, pp. 377, 378.

[11]Fletcher, C. A. J., "Negative Magnus Forces in the Critical Reynolds Number Regime," *Journal of Aircraft*, Vol. 9, No. 12, 1972, pp. 826–834.

[12]Seginer, A., and Ringel, M., "Magnus Effects at High Angles of Attack and Critical Reynolds Numbers," *Journal of Spacecrafts and Rockets*, Vol. 23, No. 3, 1986, pp. 237–242.

[13]Swanson, W. M., "The Magnus Effect. A Summary of Investigations to Date," *Journal of Basic Engineering*, Vol. 83, Sept. 1961, pp. 461–470.

[14]Seginer, A., and Rosenwasser, I., "Magnus Effects on Spinning Transonic Finned Missiles," *Journal of Spacecrafts and Rockets*, Vol. 23, No. 1, 1986, pp. 31–38.

[15]Almoslino, D., and McAllister, K. W., "Water Tunnel Study of Transition Flow Around Circular Cylinders," NASA TM-85879, May 1984.